



# Semantic Document Layout Analysis of Handwritten Manuscripts

Emad Sami Jaha\*

Department of Computer Science, Faculty of Computing and Information Technology, King Abdulaziz University,  
Jeddah, 21589, Saudi Arabia

\*Corresponding Author: Emad Sami Jaha. Email: ejaha@kau.edu.sa

Received: 19 September 2022; Accepted: 22 December 2022

**Abstract:** A document layout can be more informative than merely a document's visual and structural appearance. Thus, document layout analysis (DLA) is considered a necessary prerequisite for advanced processing and detailed document image analysis to be further used in several applications and different objectives. This research extends the traditional approaches of DLA and introduces the concept of semantic document layout analysis (SDLA) by proposing a novel framework for semantic layout analysis and characterization of handwritten manuscripts. The proposed SDLA approach enables the derivation of implicit information and semantic characteristics, which can be effectively utilized in dozens of practical applications for various purposes, in a way bridging the semantic gap and providing more understandable high-level document image analysis and more invariant characterization via absolute and relative labeling. This approach is validated and evaluated on a large dataset of Arabic handwritten manuscripts comprising complex layouts. The experimental work shows promising results in terms of accurate and effective semantic characteristic-based clustering and retrieval of handwritten manuscripts. It also indicates the expected efficacy of using the capabilities of the proposed approach in automating and facilitating many functional, real-life tasks such as effort estimation and pricing of transcription or typing of such complex manuscripts.

**Keywords:** Semantic characteristics; semantic labeling; document layout analysis; semantic document layout analysis; handwritten manuscripts; clustering; retrieval; image processing; computer vision; machine learning

## 1 Introduction

Today despite the rapid growth of contemporary technologies in all life aspects, including the digital transformation of paper-based content, there is still a continuous necessity to process and analyze a renewed and endless number of scanned document images. Many of these available paper



This work is licensed under a Creative Commons Attribution 4.0 International License, which permits unrestricted use, distribution, and reproduction in any medium, provided the original work is properly cited.

documents can be rare or very valuable and likely to be complex or even handwritten, like historical and ancient manuscripts [1]. For such paper documents, the mere scanning or conversion of them to their digital image format, despite their well-known advantages, is neither sufficiently efficient nor practically useful compared with further advantages and additional facilities of their fully electronic counterparts. Since those electronic ones may enable text-based search, data mining, information retrieval, and full access or processing of all content and physical entities, i.e., text, paragraphs, text lines, words, tables, charts, blocks, graphics, figures, and others. In order to enable these advantages, the information contained in paper document images must be converted into the corresponding machine-understandable form [2]. As such, document layout analysis (DLA) is used as a standard preprocessing and an essential prerequisite for developing any document image processing and analysis system. Thus, DLA has emerged as a priority topic and active research domain [3] and has increasingly become a significant interest in numerous research studies [4–9]. DLA algorithms can be carried out top-down or bottom-up with respect to their processing order [10]. Several research explorations were carried out on complex documents [2, 11], whereas some others focused on more complex historical documents, which may implicate challenging handwritten manuscripts in different languages [12–14]. Moreover, DLA can be an even more challenging task when applied to historical handwritten documents with highly unconstrained structure and complex page layouts [15, 16], as in ancient/historical Arabic manuscripts [17–19].

Most DLA approaches share the common primary goal of physical/structural layout analysis and the initial task of simply segmenting an input document image into textual and non-textual regions [20]. While a number of those approaches undertake a further task of classifying text/non-text regions based on positional role in the document into classes like title, paragraph, header, footer, or sidenote [21], and non-text classes can be a table, figure, chart, graphic, or separator [22]. For this classification, a diversity of preliminary and sophisticated techniques of image processing, computer vision, and machine learning was effectively devoted. Consequently, various research approaches were proposed using different combinations of such functional techniques comprising: anisotropic diffusion with geometric features for historical DLA [17]; local binary pattern (LBP) for text/non-text separation of handwritten documents [4]; contour classification methods and morphological operators for the complex layout of newspapers and magazines [11]; Harris corner detectors for gradient-based manuscript segmentation and reconstruction [19]; homogeneity algorithm and mathematical morphology for page element segmentation [22]; 2D Markovian approach with supplemental textual and spatial information for handwritten letters [6]; and support vector machine (SVM) for text and metadata extraction from Arabic documents [5]. Performing consecutive or cumulative connected component (CC) and pixel analyses on a document image was a typical dominant technique enforced to initially identify regions and then classify them, as adopted by the majority of proposed DLA systems [17, 19, 22]. Furthermore, advanced deep learning models were also used for empowering different DLA frameworks [7–9, 23].

Many research studies have been conducted using DLA for document layout-based clustering, highlighting the importance and usefulness of clustering documents—depending on different common layout properties—in several practical applications [18, 24–26]. For instance, to solve the problem of non-standard and densely populated documents, a clustering algorithm combined with simple refinement rules was used to cluster some layout constituents and improve document image segmentation [9]. Furthermore, clustering documents by their types (e.g., invoices, articles, letters) is a desirable solution for archiving massive collections of scanned documents. It can be offered by exploiting layout characteristics to assist in grouping similar documents [24]. Further detailed clustering of layout elements for constructing a cluster tree to model the layout hierarchy could also be influential on

document layout understanding [25]. Nevertheless, it was found more challenging to analyze and cluster relying on a layout or its modules when document scripts are written in languages, like Arabic, with cursive writing and different styles [18].

Document retrieval is a critical capability and highly demanding task, which may often be associated with clustering as a prior stage in integrated document analysis systems. Therefore, document image retrieval (DIR) has been deemed as the primary research interest in multiple DLA-relevant studies [1,27,28]. A DIR on a layout similarity basis was proposed using regions' extraction and tree-based representation with a combination of different clustering and indexing methods, aiming to retrieve the most similar pages from sizable digital library collections [26]. String edit distance was suggested as graph-based layout matching and document retrieval [29]. Unsegmented images were used to find layout sub-region matches for scalable ranked retrieval from a large document corpus [30]. In [31], text parsing and DLA were combined to develop a gadget tool for messaging apps, allowing users to link certain document parts, e.g., figures or tables, to be instantly retrieved and displayed across their chats.

Very little research has been concerned with inferable semantic-related aspects, which are contained in analyzed document files or images [32,33]. One likely reason is that semantic analyses largely depend on the document type, which makes it challenging to produce a generalized solution of logical/semantic layout analysis able to identify inter-region relationships and realize the semantic arrangement of these regions [21]. A unified DLA framework was proposed as a multimodal analyzer for enhanced document understanding. Such that it processes both text and image formats of an input portable document format (PDF) file of a machine-written document and fuses vision-based image features with natural language processing (NLP) based text semantics, besides the relations between layout components [32]. Another study proposed a multimodal neural model for the semantic segmentation of historical newspapers by combing visual and textual features [14]. For document triage, from the semantic point of view, structural information potential (SIP) was introduced as a measure of information based on the potentiality of structures to be informative about their content [33].

The latent semanticity power is yet to be essentially investigated or mainly employed in DLA and characterization and has been unlikely to be considered by earlier related research efforts. However, the analysis, derivation, and interpretation of image semantic information were proved to be effectively valuable and successful in supplementing traditional/physical features in other computer vision-based estimation and classification problems [34,35], as well as bridging the semantic gap as a crucial problem present in most automatic image annotation (AIA) tasks and content-based image retrieval (CBIR) systems [35–37]. Hence, this research is conducted as an initial study to investigate the validity and potency of proposed semantic document layout characteristics in enabling further semantic-based capabilities and achieving improved document processes, including clustering and retrieval based on layout similarities using different combinations of the proposed semantic characteristics.

In this research, the concept of *semantic* document layout analysis (SDLA) is introduced and distinguished from the traditional well-established, and widely used standard DLA. Such automatic semantic layout analysis and characterization capabilities of complex handwritten manuscripts can be effectively utilized in dozens of practical applications and different purposes, in a way bridging the semantic gap and providing human-friendly, more understandable document analysis and characterization. Although the resulting high-level semantic characteristics describe the document layout with *absolute* and *relative* labels in a less detailed and more overview manner than the traditional or physical low-level layout features. They can be more invariant and immune to potential minor errors

or imperfect processes of detection and segmentation in the corresponding physical DLA. Unlike the majority of existing research explorations, this research effort is devoted to achieving an effective automated system for physically and *semantically* analyzing document layout of a considerable number of scanned documents of complex handwritten manuscripts in the Arabic language. The main contributions of this research can be summarized as follows:

- extending the traditional concept of document layout analysis (DLA) to the semantic domain and introducing the corresponding concept of *semantic* document layout analysis (SDLA);
- proposing a set of high-level semantic layout characteristics along with a descriptive group of *absolute* and *relative* labels for effectively characterizing a handwritten manuscript layout;
- designing a novel SDLA framework for semantic layout analysis and characterization of handwritten manuscripts, enabling automatic derivation of implicit semantic information using extended image processing, computer vision, and machine learning techniques in such a way as bridging the semantic gap; and
- conducting detailed investigation and validation of new semantic-based manuscript clustering and retrieval approaches incorporating different combinations of effective semantic characteristics and physical features.

The remainder of this paper comprises four sections. Section 2 introduces the proposed semantic layout characteristics and their descriptive absolute and relative labels. While Section 3 describes in detail the SDLA framework and methodology used in this research. Semantic-based manuscript clustering and retrieval are demonstrated in Section 4, and finally, conclusions and future work are provided in Section 5.

## 2 Semantic Layout Characteristics

Amongst many possible document layout characteristics, an initial set is adopted for this research study comprising those which appear to be fundamental, generic, and more suited for semantically characterizing a handwritten manuscript or document. As such, the set of characteristics is chosen and defined in a top-down manner, starting with semantically describing the overall aspects of the manuscript, then gradually describing the underlying non-textual/textual content and components. This set of characteristics is considered to be as much as possible structural, comprehensive, observable, conventional, and understandable. In this research, the proposed semantic layout characteristics differently describe the manuscript using absolute and relative groups of labels, where a single characteristic can be described using either or both types of labels. [Table 1](#) shows the proposed list of semantic layout characteristics with their assigned absolute and relative labels. Note that fifteen characteristics are shown in bold as they are relatively describable with relative labels.

**Table 1:** Semantic document layout characteristics and corresponding labels

Doc. aspect	ID	Semantic characteristic	Absolute labels	Relative labels
<i>Page overall</i>	C1	Orientation	[Portrait, Landscape]	-
	C2	Page layout	[Single-page, Double-page]	-
	<b>C3</b>	<b>Margins</b>	[None, Asymmetric, Horizontal-symmetric, Vertical-symmetric, Symmetric]	[None, Narrow, Moderate, Wide]

(Continued)

**Table 1:** Continued

Doc. aspect	ID	Semantic characteristic	Absolute labels	Relative labels
<i>Non-textual objects</i>	<b>C4</b>	<b>Non-text</b>	[Absent, Present]	[None, Very low, Low, Medium, High, Very high]
	<b>C5</b>	<b>Scribble</b>	[Absent, Present]	[None, Very low, Low, Medium, High, Very high]
<i>Text layout</i>	<b>C6</b>	<b>Page lines</b>	[Absent, Present]	[None, Few, Moderate, Many]
	<b>C7</b>	<b>Title</b>	[Absent, Present]	-
	<b>C8</b>	<b>Miscellaneous text</b>	[None, Single, Double, Multiple]	-
	<b>C9</b>	<b>Paragraph</b>	[None, Single, Double, Multiple]	-
	<b>C10</b>	<b>Text-lines</b>	[None, Single, Double, Multiple]	[None, Few, Moderate, Many]
	<b>C11</b>	<b>Avg. line spacing</b>	[None, Tight, Single, Double, Multiple]	[None, Narrow, Moderate, Wide]
	<b>C12</b>	<b>Avg. paragraph spacing</b>	[None, Tight, Single, Double, Multiple]	[None, Narrow, Moderate, Wide]
	<b>C13</b>	<b>Baseline quality</b>	[None, Winding, Ascending, Descending, Straight]	[None, Very low, Low, Medium, High, Very high]
	<b>C14</b>	<b>Alignment</b>	[None, Random, Left, Center, Right, Justified]	[None, Very low, Low, Medium, High, Very high]
	<i>Text details</i>	<b>C15</b>	<b>Text intensity</b>	-
<b>C16</b>		<b>Word density</b>	-	[None, Very low, Low, Medium, High, Very high]
<b>C17</b>		<b>Avg. lines per paragraph</b>	-	[None, Very low, Low, Medium, High, Very high]
<b>C18</b>		<b>Avg. words per paragraph</b>	-	[None, Very low, Low, Medium, High, Very high]
<b>C19</b>		<b>Size consistency</b>	-	[None, Very low, Low, Medium, High, Very high]
<b>C20</b>		<b>Text complexity</b>	-	[None, Very low, Low, Medium, High, Very high]

### 2.1 Semantic Absolute Labeling

A semantic layout characteristic can be described with a group of applicable *absolute* labels. The group of absolute labels can be defined as any conventional or nominal descriptions used to characterize that semantic characteristic. For example, the labels ('Single-page,' 'Double-page') can be used as absolute descriptions for the characteristic 'Page layout.' Note that the group of absolute labels can be in any order as they are consistently represented and used for labeling since they are merely nominal descriptions and not reflecting any measurements or ordering. Each absolute label is assigned an integer number ranging from 0 to 5 to be used as the corresponding numeric representation of that label.

## 2.2 Semantic Relative Labeling

A semantic layout characteristic can also be *relative* if it is measurable and can be described by its degree of presence/strength. Therefore, it can be described with a group of descriptive relative labels. The group of relative labels can be defined as any conventional or ordinal descriptions used to relatively characterize that semantic characteristic, such as the labels ('None,' 'Narrow,' 'Moderate,' 'Wide') can be used as relative descriptions for the characteristic 'Margins' of the manuscript. Note that the group of relative labels must be ascendingly or descendingly ordered since they are ordinal descriptions reflecting the degree of measurement or ordering. Each relative label is assigned an integer number ranging from 0 to 5, based on its order or scale in the label group, to be used as the corresponding numeric representation of that label.

## 3 Research Methodology

The proposed research methodology based on a framework constitutes of a number of phases starting with using a raw manuscript document as an input to the preprocessing phase, followed by the main processing phase of semantic layout analysis and characterization, and ending with the phase of semantic modeling and nascent capabilities of semantic-based clustering and retrieval. The vital phase of the proposed framework is the semantic layout analysis and characterization phase, designated for semantic characteristic extraction and labeling. This phase comprises four modules: analyzing the page overall, analyzing non-textual objects, analyzing text layout, and analyzing text details. Fig. 1 presents an overview of the proposed framework for SDLA and the characterization of complex manuscripts.

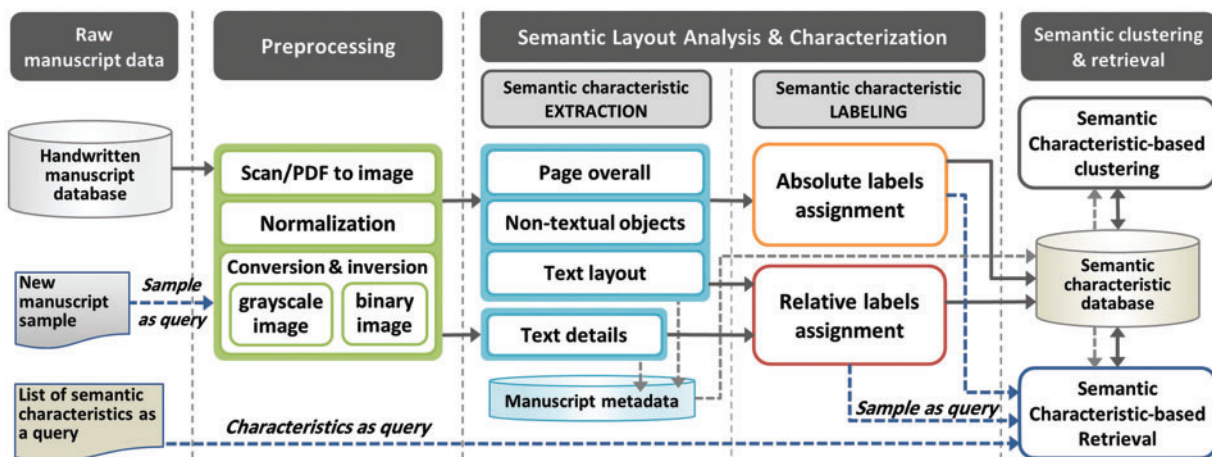


**Figure 1:** SDLA framework for semantic layout analysis and characterization of handwritten manuscripts

### 3.1 Handwritten Manuscript Database

In this research, the proposed experimental work is conducted using a large complex document database consisting of 44968 scanned Arabic manuscripts in PDF format, while 27604 are mostly double-page landscape manuscripts resulting in over 70000 pages when added to the remaining portrait single-page manuscripts. All manuscripts were handwritten over around ten years by multiple cooperated authors and ended up with a single encyclopedia specialized in interpreting and studying the Holy Quran text on different levels, including word, verse (ayah), section, and chapter (surah).



This raw database was originally divided per chapter (surah) into 114 groups. Each group included a set of related manuscripts, and each manuscript belonged to one of the four categories of study (i.e., word, verse, section, and chapter). Nevertheless, here the whole manuscript data is reorganized and divided into five datasets based on the four categories mentioned above and an additional fifth category comprising 44 manuscripts of the encyclopedia introduction. Table 2 shows a summary of the handwritten manuscript database and the implied five datasets of different categories, while Fig. 2 shows a data sample of each of these five manuscript categories.

**Table 2:** Handwritten manuscript database description

Dataset name	Number of documents	Category	Content description
Dataset-1	27604	Word study	Studying the Quranic utterances (Alfaz) and words (Kalimat)
Dataset-2	6394	Verse study	Studying the Quranic verse (Ayah)
Dataset-3	10754	Section study	Studying the Quranic section (Maktaa’)
Dataset-4	172	Chapter study	Studying the Quranic chapter (Surah)
Dataset-5	44	Introduction	Introducing the Quranic encyclopedia basics/terminology
Total	44968		

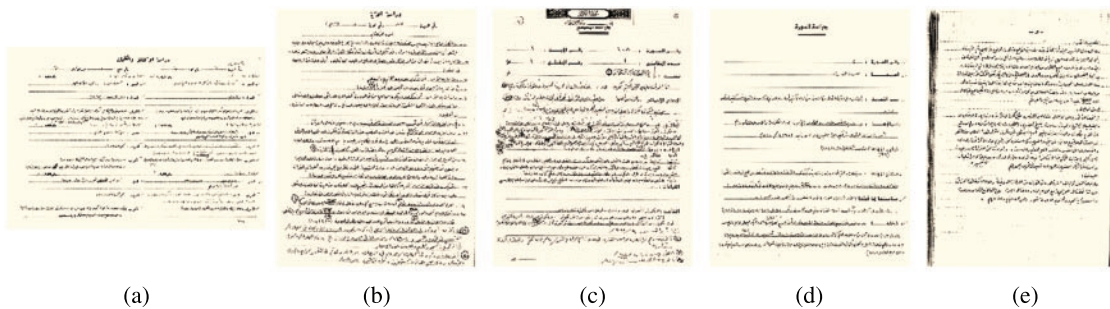


**Figure 2:** A data sample of each of the five manuscript categories listed in Table 2, respectively

### 3.2 Preprocessing

Each manuscript is initially passed through a preprocessing stage, starting with converting the PDF file to a joint photographic expert group (JPEG) image format for further required image processing and computer vision-based analysis. This conversion is automatically applied with the highest JPEG quality to an input PDF document using a programmer-friendly convert document to image (CDTI) tool by SoftInterface. The resulting manuscript image is normalized in such a way as to maintain the aspect ratio based on the initial image width ( $w_0$ ) or height ( $h_0$ ). If  $w_0 \leq h_0$ , then  $h_0$  is resized to a predefined normalized height as  $h_0 = h_{norm}$ , and  $w_0$  is accordingly resized relatively based on the new size of  $h_0$ . Whereas if  $w_0 > h_0$ , then  $w_0$  is resized to a predefined normalized width as  $w_0 = w_{norm}$ , and then  $h_0$  is accordingly resized relatively based on the new size of  $w_0$ . The normalized manuscript image  $I$  is then converted to both grayscale  $I_{gray}$  and binarized  $I_{bin}$  images, which are further inverted

and denoted as  $I'_{gray}$  and  $I'_{bin}$  respectively, such that  $I'_{gray}$  represents foreground pixels in bright gray levels and the background pixels in dark gray levels, while  $I'_{bin}$  represents the foreground and background in white and black, respectively, as shown in Fig. 3. These different forms of the normalized manuscript image are subsequently used in several CC and pixel-based analyses.

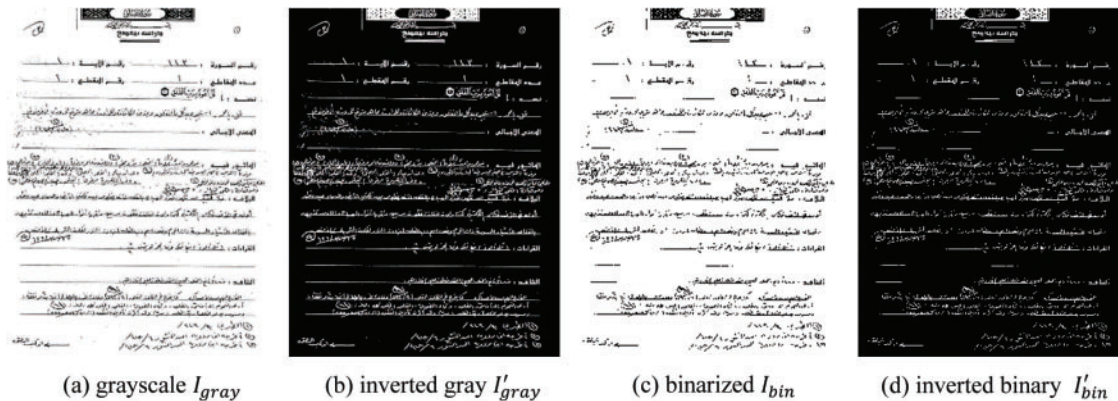


**Figure 3:** Different forms of a normalized manuscript image used for CC-/pixel-based analysis

### 3.3 Semantic Document Layout Analysis (SDLA) and Characterization

In this stage, basic and advanced image processing, computer vision, and machine learning techniques are devoted and effectively used not merely for traditional document layout analysis and segmentation but beyond that for bridging the semantic gap and achieving semantic-based layout analysis and characterization. This semantic analysis and characterization lead to generating a list of meaningful and conventional high-level descriptions to better understand and validate a document layout, especially in the case of atypical complex handwritten manuscripts. As such, for all four document aspects in Table 1, each semantic characteristic is analyzed and assigned the most suited label from the corresponding absolute/relative group of labels, using the proposed SDLA and characterization, as shown in Fig. 4.

#### 3.3.1 Analyzing Page Overall

Three semantic characteristics (C1, C2, and C3) related to the manuscript *page's overall* appearance, namely page orientation, layout, and margins, are analyzed and semantically characterized by assigning appropriate absolute or relative labels. The page 'Orientation' (C1) is detected and assigned a suitable label by simply computing the ratio between the width  $w_0$  and height  $h_0$  of the original manuscript image  $I$ , where the orientation is considered as 'Portrait' if  $w_0/h_0 \leq 1$  and 'Landscape' if  $w_0/h_0 > 1$ .

The 'Page layout' (C2) is recognized to infer the correct label by applying to the inverted binary manuscript image  $I'_{bin}$  a combination of morphological operations [2,11,17] and image CC analyses [18,20,21]. After excluding the margin and potential title zone, if any, a number of proper morphological dilation, area closing/opening, and erosion operations are performed with a proper value setting in such a way that is suited and widely applicable to most average handwritten manuscript text. Next, a vertical projection profile is performed and analyzed to clarify and detect the likely middle margin existence between two pages in a single image. These processes are used to consolidate the visually related components of the page content, resulting in either one or two large components or



blocks of (ones) white pixels in the binary image. Accordingly, assign the appropriate ‘Single-page’ or ‘double-page’ label, as illustrated in Fig. 5.

The page ‘Margins’ (C3) are analyzed and characterized differently by corresponding absolute and relative labels. Thus, the area open operation is performed on the inverted binary image  $I_{bin}^i$  for clearing or reducing unnecessary scanning noise to accomplish accurate segmentation of the content from the background [19]. Union convex hull composition methods [38,39] are adapted and applied to create a single convex hull around the content of the manuscripts. Then, the margins are estimated for all four directions (i.e., left ( $l_m$ ), right ( $r_m$ ), top ( $t_m$ ), and bottom ( $b_m$ )). Therefore, for each direction, a margin is estimated as the number of pixels in the line crossing a vertical/horizontal rectangular strip area of (zeros) black pixels and located between the image edge of that direction and the foremost point (or peak) of the union convex hull in the same direction. The margin area is the merge of all four rectangular strip areas. Hence, the absolute labeling  $\mathcal{M}_A$  is achieved as described in Eq. (1) formulation.

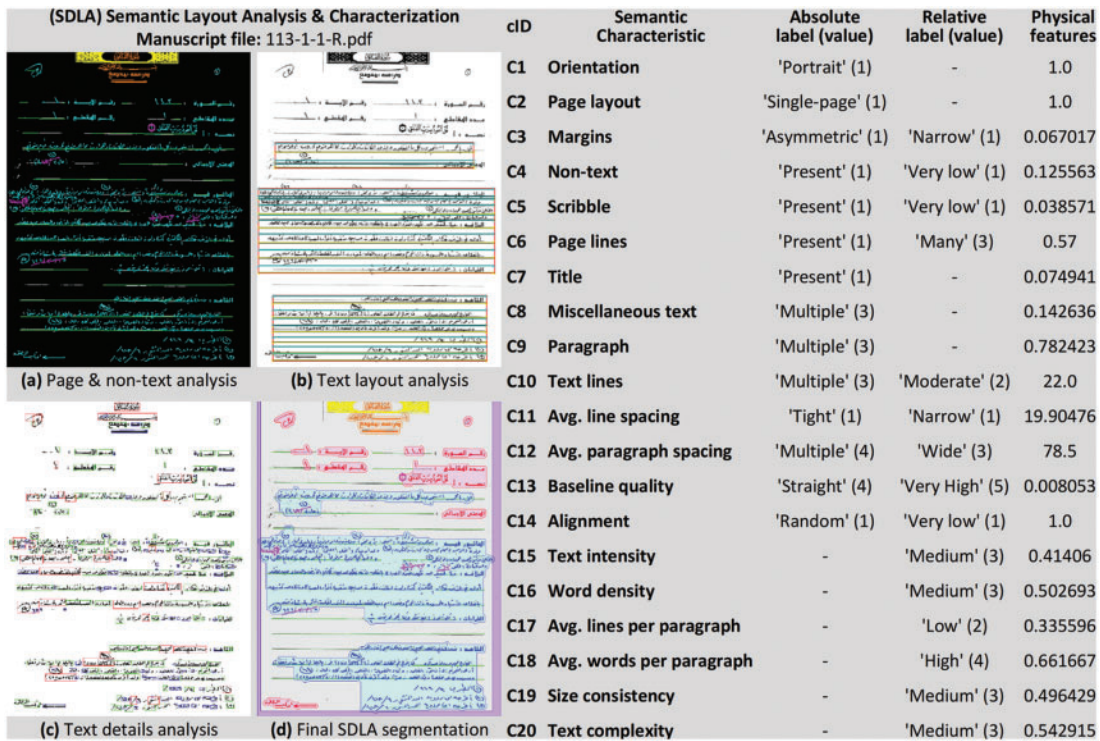


Figure 4: SDLA report of semantic layout analysis, characterization, and physical feature extraction

$$\mathcal{M}_A(l_m, r_m, t_m, b_m) = \begin{cases} 0 & \text{if } \text{sum}(l_m, r_m, t_m, b_m) = 0 \\ 1 & \text{if } |l_m - r_m| > \tau \text{ and } |t_m - b_m| > \tau \\ 2 & \text{if } |l_m - r_m| \leq \tau \text{ and } |t_m - b_m| > \tau \\ 3 & \text{if } |l_m - r_m| > \tau \text{ and } |t_m - b_m| \leq \tau \\ 4 & \text{otherwise} \end{cases} \quad (1)$$

where  $l_m$ ,  $r_m$ ,  $t_m$ , and  $b_m$  are the left, right, top, and bottom margin sizes, respectively.  $\tau$  denotes the defined threshold of approximated value indicating the max number of pixels to be tolerated as an

acceptable difference between every two opposite margins. As such, the label ‘None’ is assigned if the total of all four margin sizes calculated by the function *sum* equals 0. ‘Asymmetric’ is assigned if both differences between every two opposite margins are greater than  $t$ . However, the ‘Horizontal-symmetric’ label is assigned in case the absolute difference value between left, and right margins  $|l_m - r_m|$  is less than or equal to the threshold  $t$ , whereas the counterpart difference between the top and bottom margins  $|t_m - b_m|$  is greater than  $t$ . In contrast, if  $|t_m - b_m|$  is less than  $t$  and not  $|l_m - r_m|$  then ‘Vertical-symmetric’ is assigned instead. Otherwise, ‘Symmetric’ is assigned if both differences between every two opposite margins are less than or equal to  $t$ . On the other hand, the relative labeling  $\mathcal{M}_{\mathbb{R}}$  is attained as per the formulation in Eq. (2):

$$\mathcal{M}_{\mathbb{R}}(a_m) = \begin{cases} 0 & \text{if } a_m = 0 \\ 1 & \text{if } a_m \leq A_0 * C \\ 2 & \text{if } a_m \leq A_0 * 2C \\ 3 & \text{otherwise} \end{cases} \quad (2)$$

where  $a_m$  denotes the total area of margins as the pixel sum of all four margin areas, while  $A_0$  represents the full-page area and is computed as  $A_0 = w_0 * h_0$ , the pixel sum of the whole manuscript image  $I$ , where  $a_m \subset A_0$ .  $\mathcal{M}_{\mathbb{R}}$  assigns the label ‘None’ in case of no margins (i.e.,  $a_m = 0$ ) or instead assigns a suitable relative label ‘Narrow,’ ‘Moderate,’ or ‘Wide’ based on the comparison between  $a_m$  and a corresponding partial area of the whole page area  $A_0$  (i.e., quarter, around half, or larger than half), respectively. Then, the partial area is specified according to the multiplication of  $A_0$  by the defined constant value  $C = 0.25$  in different scales corresponding to the relative labels. The final detected margin  $a_m$  is demonstrated in Fig. 5 as yellow-colored overlaid areas.

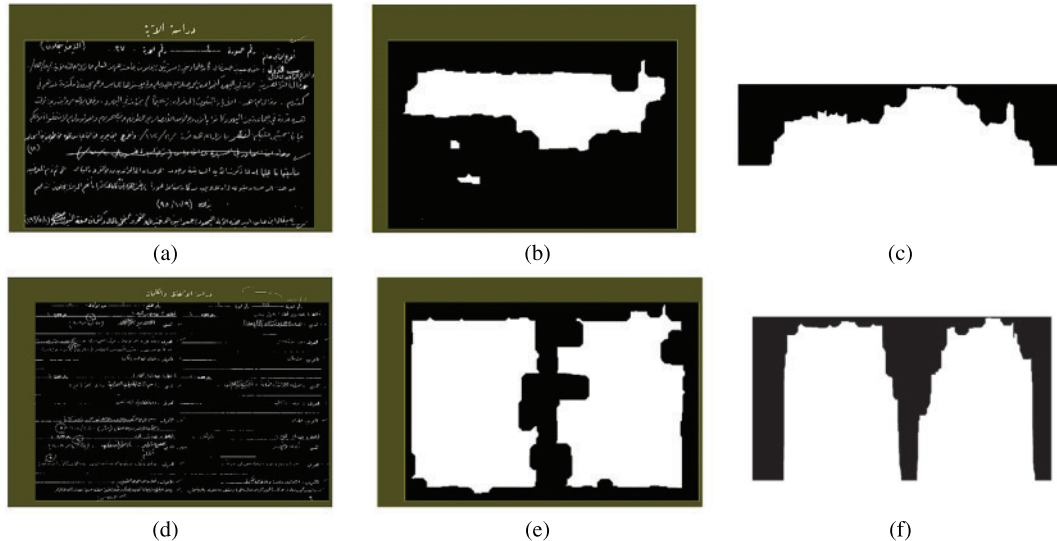


**Figure 5:** Analyzing the page’s overall semantic characteristics orientation (C1), layout (C2), and margins (C3). Processes (a–c) are for a single-page layout sample, and (d–f) for a double-page sample

### 3.3.2 Analyzing Non-Textual Objects

This semantic analyzer of *non-textual objects* is focused on characterizing objects other than texts within the manuscript content using absolute and relative descriptive labels. In particular, ‘Non-text’ (C4) objects like visual graphics or decorations, any existing ‘Scribble’ (C5) instances, and visible ‘Page

lines' (C6) captured during document scanning, as can be observed in Figs. 4a and 4d. The capability of detecting, localizing, and analyzing such objects is instrumental in simplifying manuscript complexity and enabling exclusion if needed to consequently achieve a high-quality layout analysis with accurate physical or semantic characterization.

The detection and labeling of likely 'Non-text' (C4) objects are applied to the inverted binary image  $I'_{bin}$ . A median filtering is first performed on the image to remove any noise. Next, it is followed by a smoothing process using two-dimensional convolution with a suited binary thinning filter to reduce the number of produced CCs, principally tiny or unintentional instances of unsought CCs caused by some reasons like fast handwriting or overlapping between text and page lines during the handwriting. Next, different relative thresholding methods [2,4] are used to nominate potentials and initially consider them as non-text objects, which are expected to be significantly more prominent than the average possible CC of handwritten texts. Regarding the 'Scribble' (C5) detection and characterization, a similar relative thresholding method is designed to be suited for initial scribble object detection and localization.

Before semantically labeling either non-text or scribble characteristics, each detected non-text or scribble object, as shown in magenta in Figs. 4a and 4d, is segmented. Then, it is examined using a scribble (detection) validation technique based on extracting a histogram of oriented gradient (HOG) features [35,40] along with a one-class SVM classifier [41,42]. Here the learning is achieved in a way using only positive examples [43,44], where scribble samples represent the *positive* examples, and the *negative* examples are all other non-text objects or original texts, which could be initially misdetected/misclassified as scribbles. It is perhaps due to their intersections/overlapping with visible page lines, as shown in Fig. 6.



**Figure 6:** Positive and negative scribble examples

Supposing  $X$  is the resulting HOG feature space and  $f_s$  is a scribble validation (decision) function trained to estimate a subset  $S$  of scribble objects (segments).  $f_s$  is positive in  $S$ , representing a small region capturing most of the scribble feature vectors, and negative in the complement  $\bar{S}$  representing a large area containing all (out-of-class) objects other than scribbles. As such, for a new sample  $x \in X$ , the  $f_s(x)$  value is determined, in the feature space  $H$ , by evaluating which of either positive or negative hyperplane side it falls on, such that:

$$f_s(x) = \begin{cases} +1 & \text{if } x \in S \\ -1 & \text{if } x \in \bar{S} \end{cases} \quad (3)$$

Thus, the one-class SVM training algorithm is used for mapping the data vectors into the feature space  $H$  corresponding to the kernel, then separating the mapped data vectors from the origin with the maximum margin. Hence, to achieve this separation, the following quadratic minimization problem needs to be solved:

$$\begin{aligned} & \min \left( \frac{1}{2} \|w\|^2 + \frac{1}{vn} \sum_{i=1}^n \xi_i - \rho \right) \\ & \text{subject to } (w \cdot \phi(x_i)) \geq \rho - \xi_i \quad \forall i = 1, \dots, n \\ & \xi_i \geq 0 \quad \forall i = 1, \dots, n \end{aligned} \quad (4)$$

where  $x_i$  is a feature vector example of the  $i^{\text{th}}$  scribble segment in the training set belonging to only one class  $X$ , while  $i \in n$  the total number of training examples. The nonzero slack variable  $\xi_i$  represents the training error of the  $i^{\text{th}}$  example. The separating hyperplane is determined by the two parameters  $w$  and  $\rho$ , which are meant to be found by the SVM training algorithm, where  $\|w\|^2$  characterizes the margin between positive and the origin (negative) data.  $v \in (0, 1)$  is a parameter controlling the trade-off between maximizing the margin (between the origin and the support vectors) and embracing most of the data in the region of the hyperplane with respect to the ratio of the outliers in the training dataset.  $\phi$  denotes a kernel map such that  $\phi : X \rightarrow H$ , which transforms the training examples from  $X$  feature space to another feature space  $H$ . Here, if  $w$  and  $\rho$  solve this problem of minimizing the objective function in Eq. (4), namely minimizing the training errors, and simultaneously maximizing the margin, then the following decision function

$$f_S(x) = \text{sign}((w \cdot \phi(x)) - \rho) \quad (5)$$

will be positive for most of the  $x_i$  examples in the training set. As such, if any non-text object is validated as a scribble, it is consequently eliminated from the non-text mask group and added to the scribble mask group. Only the remaining non-text objects are analyzed and considered in the semantic labeling. Thus, if no non-text objects are detected, 'Absent' and 'None' are assigned for absolute and relative labeling, respectively. In contrast, if any non-text objects are detected, 'Present' is stated as the consequent absolute label. Accordingly, the relative labeling function  $\mathcal{O}_{\mathbb{R}}$  assigns either 'Very low,' 'Low,' 'Medium,' 'High,' or 'Very high' corresponding to the proportion of  $x = x_N$  the total pixels of the non-text objects to the total pixels of all (foreground) content  $P_0$ , where  $x_N \subset P_0$ . Hence, a suited label is assigned based on the comparison with different proportional values, characterizing the relative ranges of the relative labels, where the constant  $C = 0.2$  is used in different scales to determine the corresponding proportional value of  $P_0$  for each label, as described in the formulation of Eq. (6):

$$\mathcal{O}_{\mathbb{R}}(x) = \begin{cases} 0 & \text{if } x = 0 \\ 1 & \text{if } x/P_0 \leq P_0 * C \\ 2 & \text{if } x/P_0 \leq P_0 * 2C \\ 3 & \text{if } x/P_0 \leq P_0 * 3C \\ 4 & \text{if } x/P_0 \leq P_0 * 4C \\ 5 & \text{otherwise} \end{cases} \quad (6)$$

Also, if any scribble object is invalidated as scribbles, it is excluded from the scribble mask group. Hence, only the remaining scribble objects are analyzed and semantically labeled using the same absolute and relative labeling methods used for non-text objects and described in Eq. (6). However, the relative labeling function  $\mathcal{O}_{\mathbb{R}}$ , instead, assigns an appropriate label corresponding to the proportion of  $x = x_S$  the total pixels of the scribble objects to the total pixels of all (foreground) content  $P_0$ , where  $x_S \subset P_0$ .

After excluding detected non-text and scribble objects from the manuscript, the 'Page lines' (C6) characteristic is analyzed using the inverted grayscale image  $I'_{gray}$  after performing gamma correction to enhance the luminance and contrast, allowing for sharper and more detectable page lines. The resulting image is used for page lines' detection and localization using a gradient-based Hough

transform method [45] that is modified and extended to generate a binary mask of detected page lines for segmentation and analysis. Thereby the absolute label ‘Present’ is assigned if any page lines are detected. Otherwise, ‘Absent’ is assigned instead, and accordingly, ‘None’ is assigned for relative description. Note that additional post-processing is enforced on the detected line segments to validate and verify their potentiality as page lines and to avoid misdetection of other possible random lines, utilizing some pre-knowledge about common page lines attributes such as likely ranges of line orientation, length, and position with respect to the page and texts. Then, the segmented page lines are counted and relatively thresholded to assign an appropriate relative label. Regardless of whether those detected page lines are consecutive or spread out across the page, the suited label is assigned with respect to the estimated amount of the page area where they can be regularly distributed along as in average standard page lines. Therefore, ‘Few’ is assigned if the estimated amount is less than or equal to 0.3 of the page area  $A_0$ , ‘Moderate’ if less than or equal to 0.6, and ‘Many’ if greater than 0.6.

### 3.3.3 Analyzing Text Layout

From a high-level perspective, eight semantic characteristics (C7 to C14) describing *text layout*, in general, are analyzed and labeled here, as shown in Fig. 4. For ‘Title’ (C7) detection, a title segment (if any) is localized within an expected title zone. The title zone is relatively deduced in manuscript image  $I$  on the top center of the image, excluding the top margin strip. The title zone is located right below the lower edge of the top margin  $t_m$  (inferred earlier for C3 in Section 3.3.1). As such, the title zone is deduced as a rectangular area defined by the two points  $p = (w_0/4, t_m)$  and  $q = (3w_0/4, h_0/8)$ , where  $w_0$  and  $h_0$  are the full manuscript image  $I$  width and height, respectively. Any previously detected non-text or scribble segments are eliminated if located entirely or partly within the title zone to avoid misdetection. Then, proper image filtering and morphological closing are used on the resultant binary image to remove holes and merge close textual objects, which end up with very few CCs. Thus, the absolute label ‘Present’ is stated only if a title segment is detected and localized within the title zone and sufficiently satisfies the following conditions: to be wholly or predominantly contained by the title zone; to be as a group of convergent components; to be reasonably centered along the width of the image unlike continuous sentences of a paragraph; to be notably independent or adequately isolated from other irrelevant surrounding components. Otherwise, the absolute label ‘Absent’ is assigned.

The same analysis and characterization approaches are used for both ‘Miscellaneous text’ (C8) and ‘Paragraph’ (C9). The process first starts with the inverted binary image  $I'_{bin}$ , by masking the image and removing any detected title segment besides all previously detected other non-textual objects, including non-texts, scribbles, and page lines. Secondly, an appropriate combination of morphological operations, mainly comprising dilation and closing operators, is used as a preliminary step to the detection, localization, and segmentation of nascent large CCs representing  $n$  paragraphs or other miscellaneous textual components. Thirdly, the width  $x$  of each component is standardized using z-score normalization to compute  $x' = (x - \bar{x})/\sigma$ , where  $\bar{x}$  and  $\sigma$  are, respectively, the mean and standard deviation of all widths. Then the classification is attained for each  $x$  via thresholding by half of the maximum normalized width, such that if  $x \geq \max(x')/2$ . The instance is classified as a paragraph and otherwise is classified as a miscellaneous text, where a binary mask is composed for each class consisting of all its components. Eventually, for either (C8) or (C9) characteristics, the semantic labeler assigns the absolute label ‘Single’ if only one instance is detected, ‘Double’ if two instances are detected, and ‘Multiple’ if the number of detected instances is three or more. Otherwise, ‘None’ is assigned in case no compatible objects are detected.

The ‘Text-lines’ (C10) characterization is achieved by processing and analyzing the inverted binary image  $I'_{bin}$ . A horizontal projection profile is performed on the image pixels to highlight likely



textual line segments. The ridges of the maximum values are considered the baselines of the text, and the furrows of the minimum values are deemed as spaces between text lines. Due to the nature of handwriting variance and variability, especially in the case of minimal spacing between handwritten text lines, this may cause some overlapping between letter edges of two top-bottom adjacent text lines. Therefore, it is often unlikely to detect (at least) one clear row of blank pixels, which signifies the (spacing) separation between two adjacent text lines. Thus, the resultant projection values are thresholded to the mean of all projection values, where all values less than the threshold are considered blank pixels for separating the text lines. Note that the upper and lower boundaries of the text-line projections are shifted up and down, respectively, by five pixels to fit better the text-line segment. Whereas, in case of overlapping between two top-bottom adjacent text-line segments after widening and shifting any of their upper/lower boundaries, those boundaries are shifted back to be aligned rather than overlapped. The upper and lower boundary pixels are identified for each text line and used in turn for segmenting all text lines to be further counted and semantically labeled with a suitable absolute label, where ‘Single,’ ‘Double,’ or ‘Multiple’ are, respectively assigned when one, two, three or more text-line instances are detected. Otherwise, ‘None’ is assigned instead, signifying zero text lines are detected. Furthermore, the total height of all detected  $M$  text-line instances in the manuscript is computed as  $\sum_{j=1}^M h_{\ell_j}$  for all  $j = 1, \dots, M$  the number of text-line instances, then the percent of the total text-line height to the entire manuscript height  $h_0$  is deduced as  $h'_\ell = (\sum_{j=1}^M h_{\ell_j}) / h_0$ . After that, for relative labeling purposes, ‘Few’ is assigned if the estimated percent is less than or equal to 0.25 as a quarter of the page height, ‘Moderate’ if less than or equal to 0.5 as a half of the page height, and ‘Many’ if greater than 0.5. ‘None’ is otherwise assigned, indicating no detected text lines.

The analysis of the text lines (C10) is, in turn, exploited to characterize ‘Avg. line spacing’ (C11), since the identified upper and lower boundary pixels for each line segment  $\ell$  are used once again for inferring the length of the blank space between every two lines in the same paragraph, as the distance  $d_\ell$  between the lower boundary of a text-line and the upper boundary of the next text-line (underneath). Then, the average line spacing is computed as  $\bar{d}_\ell = (\sum_{j=1}^{M-n} d_{\ell_j}) / (M-n)$ , where  $(M-n)$  is the number of spaces between  $M$  text lines excluding the last text-line from each of all  $n$  paragraphs (subject to  $n \geq 1$ ), to be compared against a scalable threshold value based on the average height  $\bar{h}_\ell = (\sum_{j=1}^M h_{\ell_j}) / M$  of all  $m$  text-line segments, where the height  $h_\ell$  of a text-line is computed as the distance between the upper and lower boundary pixels of the text-line segment. As such, for  $\bar{d} = \bar{d}_\ell$ , the absolute labeling function for spacing  $\mathcal{S}_\mathbb{A}$  can be formulated as follows:

$$\mathcal{S}_\mathbb{A}(d) = \begin{cases} 0 & \text{if } \bar{d} = 0 \\ 1 & \text{if } \bar{d} \leq \bar{h}_\ell \\ 2 & \text{if } \bar{d} \leq 2\bar{h}_\ell \\ 3 & \text{if } \bar{d} \leq 3\bar{h}_\ell \\ 4 & \text{otherwise} \end{cases} \quad (7)$$

While the relative labeling function for spacing  $\mathcal{S}_\mathbb{R}$  can be formulated as follows:

$$\mathcal{S}_\mathbb{R}(d) = \begin{cases} 0 & \text{if } \bar{d} = 0 \\ 1 & \text{if } \bar{d} \leq 2\bar{h}_\ell \\ 2 & \text{if } \bar{d} \leq 3\bar{h}_\ell \\ 3 & \text{otherwise} \end{cases} \quad (8)$$

Likewise, the analyses of (C9) and (C10), along with the labeling functions in Eqs. (7) and (8), are also utilized for achieving ‘Avg. paragraph spacing’ (C12), such that the upper and lower boundary pixels are identified for each paragraph segment  $p$  detected for (C9) using the same method used

with the text-line segments. This is for inferring the length of the blank space between every two paragraphs, as the distance  $d_p$  between the lower boundary of a paragraph and the upper boundary of the next paragraph (underneath). Then, the average paragraph spacing is computed for  $\bar{d} = \bar{d}_p = \left( \sum_{i=1}^{n-1} d_{pi} \right) / (n - 1)$ , where  $(n - 1)$  is the number of spaces between  $n$  paragraphs (subject to  $n \geq 2$ ), to be then compared against the same scalable threshold value based on the average height  $\bar{h}_\ell$  of all text-line segments, as used for (C11).

Consequently, for both (C11) and (C12), a suitable absolute label of ‘Tight,’ ‘Single,’ ‘Double,’ or ‘Multiple’ is assigned based on a comparison of spacing when the function in Eq. (7) value equals (1, 2, 3, or 4), respectively, which corresponds to single, double, triple, or more than triple of the average text-line height. Furthermore, a relative label of ‘Narrow,’ ‘Moderate,’ or ‘Wide’ is assigned based on a comparison of spacing when the function in Eq. (8) value equals (1, 2, or 3), respectively, which corresponds to an average spacing less than or equal double, triple, or more than triple of the average text-line height  $\bar{h}_\ell$ . However, ‘None’ is assigned for both absolute and relative labeling if there are no text lines or only one text line or paragraph segment exists, or no spaces are detected.

The manuscript’s paragraphs, detected for (C9), are further analyzed in terms of ‘Baseline quality’ (C13) and characterized using applicable absolute/relative labeling, where the baseline here is estimated and analyzed with respect to a whole text line only within a paragraph. The inverted binary image  $I'_{bin}$  is used in this analysis such that, among all text lines detected for (C10), only those located within paragraphs are analyzed, and some effective morphological operations are used to primarily reform each text-line  $\ell_{ij}$  as a single CC, where  $\ell_{ij}$  is the  $j^{\text{th}}$  text-line of the  $i^{\text{th}}$  paragraph  $p_i$ . This, in turn, enables measuring the text-line orientation  $\theta_{ij}$  of the main skeleton line of the convex hull deduced for the resulting CC. Consequently, for all text lines  $M = \sum_{i=1}^n m_i$  within all  $n$  paragraphs, the average orientation is inferred as  $\bar{\theta} = \left( \sum_{i=1}^n \sum_{j=1}^{m_i} \theta_{ij} \right) / M$ , where  $m_i$  is the number of text lines in the  $i^{\text{th}}$  paragraph  $p_i \forall i = 1, \dots, n$ .

In addition, a baseline estimation method inspired by [46] is used but per the whole text line rather than per word or sub-word. Hence, the original inverted binary image  $I'_{bin}$  is used for computing the horizontal projection of the skeleton of those text lines after filtering out tiny objects like dots and noises, and thereby the baseline is measured as the highest peak of the horizontal projection of the whole text line. However, if more than nonadjacent peaks are detected with very similar values (with  $\pm 2$  tolerance rate), the text line is considered as winding (or wavy), and the counter  $c$  of winding text lines is increased by one. The percentage of winding text lines to the entire text lines is inferred as  $c' = c/M$ . Eventually, the labeling is achieved by the following absolute  $\mathcal{B}_A$  and relative  $\mathcal{B}_R$  formulations:

$$\mathcal{B}_A(\bar{\theta}, c') = \begin{cases} 0 & \text{if } n = 0 \\ 1 & \text{if } c' \geq 0.4 \\ 2 & \text{if } \bar{\theta} < -2^\circ \\ 3 & \text{if } \bar{\theta} > 2^\circ \\ 4 & \text{if } -2^\circ \leq \bar{\theta} \leq 2^\circ \end{cases} \quad (9)$$

$$\mathcal{B}_{\mathbb{R}}(\bar{\theta}, c') = \begin{cases} 0 & \text{if } n = 0 \\ 1 & \text{if } c' \geq 0.4 \text{ or } \bar{\theta} < -2^\circ \text{ or } \bar{\theta} > 2^\circ \\ 2 & \text{if } -2^\circ \leq \bar{\theta} < -1.5^\circ \text{ or } 1.5^\circ < \bar{\theta} \leq 2^\circ \\ 3 & \text{if } -1.5^\circ \leq \bar{\theta} < -1^\circ \text{ or } 1^\circ < \bar{\theta} \leq 1.5^\circ \\ 4 & \text{if } -1^\circ \leq \bar{\theta} < -0.5^\circ \text{ or } 0.5^\circ < \bar{\theta} \leq 1^\circ \\ 5 & \text{if } -0.5^\circ \leq \bar{\theta} \leq 0.5^\circ \end{cases} \quad (10)$$

As such, ‘None’ is stated as the absolute and relative labels when  $n = 0$ , namely, no existing paragraphs. Alternatively, for absolute labeling, the  $\mathcal{B}_{\mathbb{A}}$  values (1, 2, 3, and 4) as in Eq. (9) correspond to the labels ‘Winding,’ ‘Ascending,’ ‘Descending,’ and ‘Straight,’ respectively, whereas, for relative labeling, the  $\mathcal{B}_{\mathbb{R}}$  values (1, 2, 3, 4 and 5) as in Eq. (10) reflect the labels ‘Very low,’ ‘Low,’ ‘Medium,’ ‘High,’ and ‘Very high,’ respectively. Note that the negative values of  $\bar{\theta}$  angles indicate ascending baseline, and positive values indicate descending since the used (Arabic) manuscripts are written in a right-to-left direction here.

For characterizing the overall text ‘Alignment’ (C14), all paragraph and text-line segments, derived previously for (C9) and (C10), are evaluated here to assign the most descriptive absolute and relative labels. It is noteworthy that the first and last lines of a paragraph may have a different appearance than the other in-between lines, and some exceptional cases need to be considered in analyzing and classifying the alignment style, such as first-line indention and incomplete last line, which can be expected in all standard alignment styles, i.e., left, right, center, or justified. Therefore, ‘None’ is assigned for both absolute and relative labeling once no paragraphs are detected, as for (C9). However, if ‘None’ is not the applicable absolute/relative label, the following algorithm is used for text alignment analysis and assignment of the other applicable labels.

### 3.3.4 Analyzing Text Details

Further characteristics (C15 to C20) representing some different *text details* are semantically analyzed (See Fig. 4) and only relatively described, each using an applicable label of (‘None,’ ‘Very low,’ ‘Low,’ ‘Medium,’ ‘High,’ and ‘Very high’) according to the comparison between a proportional value deduced by  $f(x)$  and a multi-scale threshold  $t$  characterized by a variable  $\nu$  and constant value  $C$ , where  $C$  is mostly set to 0.2 (or 1/5) to specify the minimum range of the threshold scale defined by  $\nu$  and also used as a step size of the bipolar five-point scaler ranging from ‘Very low’ to ‘Very high.’ A generic labeling formulation of text details characteristics can be defined as follows:

$$\mathcal{L}_{\mathbb{R}}(x) = \begin{cases} 0 & \text{if } f(x) = 0 \\ 1 & \text{if } f(x) \leq t \\ 2 & \text{if } f(x) \leq 2t \\ 3 & \text{if } f(x) \leq 3t \\ 4 & \text{if } f(x) \leq 4t \\ 5 & \text{otherwise} \end{cases} \quad (11)$$

where

$$t = \nu * C \text{ subject to } \nu > 0, C > 0 \quad (12)$$

The ‘Text intensity’ (C15) characteristic is deduced as  $f(x) = \sum_N x$ , the pixel sum for all the  $N$  number of the pure text pixels in the inverted binary image  $I'_{bin}$ , excluding all non-textual components.

**Algorithm of C14**

- 
1. Let  $p_i$  be the inferred rectangular bounding box of the  $i^{\text{th}}$  paragraph in a manuscript containing  $n$  number of paragraphs, where  $i = 1, \dots, n$ ;  
 let  $\ell_{ij}$  be the inferred rectangular bounding box of the  $j^{\text{th}}$  text-line located within the  $i^{\text{th}}$  paragraph  $p_i$  comprising  $m_i$  number of text lines, where  $j = 1, \dots, m_i$ ;  
 let  $L$  and  $R$  be symbols indicate respectively the left-side and the right-side of any bounding-box  $p_i$  or  $\ell_{ij}$ ;  
 let  $|d_{ijL}|$  be the absolute value of the left-side distance between  $p_{iL}$  and  $\ell_{ijL}$ ; and  $|d_{ijR}|$  be the absolute value of the right-side distance between  $p_{iR}$  and  $\ell_{ijR}$ ; and  
 let  $\mathcal{A}_i$  be the text alinement absolute sub-label of the paragraph  $p_i$ ; and  
 let  $D_{\Delta}$  be the dominant and most frequent absolute sub-label  $\mathcal{A}_i$  and  $F_{\Delta}$  be the frequency value of  $D_{\Delta}$   
 let  $D_{\mathbb{R}}$  be the relative label corresponding to  $D_{\Delta}$  along with  $F_{\Delta}$
  2. For each  $p_i$  compute  $|d_{ijL}|$  between  $p_{iL}$  and each  $\ell_{ijL}$ ; and compute  $|d_{ijR}|$  between  $p_{iR}$  and each  $\ell_{ijR}$
  3. For each  $p_i$ , if all  $|d_{ijL}| \approx 0, \forall j = 2, \dots, m_i$  and any  $|d_{ijR}| > 0, \forall j = 1, \dots, (m_i - 1)$ , then set  $\mathcal{A}_i$  as ‘Left’; else  
 if all  $|d_{ijR}| \approx 0, \forall j = 2, \dots, m_i$  and any  $|d_{ijL}| > 0, \forall j = 1, \dots, (m_i - 1)$ , then set  $\mathcal{A}_i$  as ‘Right’; else  
 if all  $|d_{ijL}| \sim |d_{ijR}|, \forall j = 1, \dots, m_i$  and any  $|d_{ijL}| \sim |d_{ijR}| > 0, \forall j = 1, \dots, m_i$ , then set  $\mathcal{A}_i$  as ‘Center’; else  
 if all  $|d_{ijL}| \approx |d_{ijR}| \approx 0, \forall j = 1, \dots, j \geq (m_i - 1)$  and for the last text lines  $|d_{im_iL}| \approx 0$  and  $|d_{im_iR}| > 0$  or vice-versa, then set  $\mathcal{A}_i$  as ‘Justified’; else set  $\mathcal{A}_i$  as ‘Random’
  4. Find  $D_{\Delta}$  and  $F_{\Delta}$  from all assigned sub-labels of  $\mathcal{A}_i \in$  (‘Random,’ ‘Left,’ ‘center,’ ‘Right,’ ‘Justified’)
  5. If  $F_{\Delta} \gtrsim \frac{3}{5}n$ , consider the current  $D_{\Delta}$  as the overall alinement absolute label of  $p_i$ . Otherwise, set  $D_{\Delta}$  as ‘Random’
  6. If  $D_{\Delta}$  is ‘Random,’ set  $D_{\mathbb{R}}$  to ‘Very low’; else if  $D_{\Delta}$  is ‘Center,’ set  $D_{\mathbb{R}}$  to ‘low’; else if  $D_{\Delta}$  is ‘Justified,’ set  $D_{\mathbb{R}}$  to ‘Very high’; else if  $D_{\Delta}$  is ‘Left’ or ‘Right’ then: If  $F_{\Delta} \lesssim \frac{4}{5}n$  set  $D_{\mathbb{R}}$  to ‘Medium’; else set  $D_{\mathbb{R}}$  to ‘high’
- 

Accordingly,  $\tau$  is computed by multiplying  $C = 0.2$ , and a predefined value of  $v$  is inferred as a maximal pixel sum of a manuscript fully filled with handwritten text with minimal line spacing. Then,  $\tau$  is used for comparison and thresholding in different scales corresponding to the different relative labels, where the values (0, 1, 2, 3, 4, and 5) are the numeral representation of the relative labels (‘None,’ ‘Very low,’ ‘Low,’ ‘Medium,’ ‘High,’ and ‘Very high’), respectively.

For analyzing and labeling the ‘Word density’ (C16) characteristic, the inverted binary image  $I'_{bin}$  is masked to maintain only the pure textual content. Then a morphological closing operation is used in such a way suited for merging the sub-words or letters per word to mainly reform it as one CC representing a single word. Morphological opening operation is next applied to the nascent image to eliminate noise and unnecessary fragments. Subsequently, words are segmented and counted as  $k$  to assign the value of  $x = k$  and achieve semantic labeling  $\mathcal{L}_{\mathbb{R}}(x)$  as in Eq. (11). A rectangular bounding box is inferred for each word segment  $\omega$  and the average box area  $\bar{\omega} = \left(\sum_{u=1}^k \omega_u\right) / k$  is calculated of all  $k$  (word) bounding boxes. So, the ratio of  $x$  to a proportional value is computed, such that  $f(x) = x / (A_0 / \bar{\omega}) * 0.4$  where  $x$  is the number of detected  $k$  words and  $A_0$  is the total (manuscript) image area, as  $A_0 / \bar{\omega}$  can be described as the number of average (word) bounding box  $\bar{\omega}$  that can be

fit within 0.4 of the (manuscript) image area  $A_0$ , where  $A_0$  was computed and used earlier for (C3) in Section 3.3.1. Moreover, based on  $\nu = 1$  and  $C = 0.2$ ,  $t$  is computed for multi-scale thresholding and relative labeling of estimated word density.

Each paragraph segment, detected earlier for (C9 in Section 3.3.3), is segmented into text lines and words for further semantic analysis to characterize the ‘Avg. lines per paragraph’ (C17) and ‘Avg. words per paragraph’ (C18). The text-line segmentation is attained using the exact mechanism of the horizontal projection profile used with overall manuscript text lines (C10), but per paragraph segment instead. The exact word detection and localization technique used for (C16) is utilized here for word segmentation and counting within each paragraph segment as an area of interest instead of the overall manuscript.

For (C17) labeling, the average number of lines per paragraph is computed as  $f(x) = (\sum_{i=1}^n x_i)/n$ , where  $n$  is the number of paragraphs in the manuscript and  $x_i$  is the number of text lines in the  $i^{\text{th}}$  paragraph. The resulting average is relatively thresholded to  $t$  characterized by  $C = 0.2$  and  $\nu$  that represents here the max number of text lines with height equals the average text-line height  $\bar{h}_\ell$  that can be stacked along 0.4 of the manuscript height  $h_0$  excluding the top  $t_m$  and bottom  $b_m$  margins, such that  $\nu = 0.4 * (h_0 - (t_m + b_m))/\bar{h}_\ell$ , where all values of these variables were derived and used in earlier processes of (C1 and C3 in Section 3.3.1, and C12 in Section 3.3.3). The compatible relative label is determined by Eq. (11).

For (C18) labeling, the average number of words per paragraph is computed using  $f(x) = (\sum_{i=1}^n x_i)/n$ , where  $n$  is the number of paragraphs and  $x_i$  here is the number of words in the  $i^{\text{th}}$  paragraph. The resultant average is relatively thresholded to  $t$  characterized by  $C = 0.2$ , and  $\nu$  derived as the max number of words with an area equals the average (word) bounding box area  $\bar{w}$  that can be fit within half of the average paragraph area computed as  $\bar{p} = (\sum_{i=1}^n p_i)/n$ , such that  $\nu = \frac{1}{2} (\bar{p}/\bar{w})$ , where  $\bar{w}$  was already derived and used in earlier processes of (C16) and the multiplication by  $1/2$  is to reflect the nature of spaces between text lines and words when fitting the max number of the average word  $\bar{w}$  within the average paragraph  $\bar{p}$ . Thereafter, the obtained value of Eq. (11) determines the consequent relative label.

The text ‘Size consistency’ (19) in the case of handwriting, which is unlikely to be as high as in the case of machine-written documents, is explored and analyzed by utilizing all segmented text lines and words along with their inferred rectangular bounding boxes, as derived earlier for (C10 in Section 3.3.3, and C16). Since the width of words is naturally anticipated to vary highly from one to another based on shape, width, and the number of their composing letters, especially in such cursive Arabic scripts used in this research, the height of words is, therefore, supposed (and deemed as a desirable characteristic of good handwriting) to maintain some consistency and appears with a notable baseline and virtual upper and lower bounds conceptualizing the upper and lower limits of words within a text-line. Thus, the mean height  $\bar{h}_\ell$  and the standard deviation  $\sigma_\ell$  are derived from all manuscript text-line bounding boxes to be used to evaluate the height of each word bounding box  $h_{w_u}$  ( $\forall u = 1, \dots, k$  the total number of words) to find and count the number of word outliers of the consistent word height (or size) range. Each word height  $h_{w_u}$  is compared with respect to height and considered as an outlier  $\varepsilon_u = 1$  and added to the sum of all outliers  $\sum_{u=1}^k \varepsilon_u$  such that:

$$\varepsilon_u = \begin{cases} 0 & \text{if } (\bar{h}_\ell/2 + \sigma_\ell/2) \leq h_{w_u} \leq \bar{h}_\ell \\ 1 & \text{otherwise} \end{cases} \quad (13)$$

By using the labeling function in Eq. (11) with Eq. (12),  $f(x) = k - \sum_{u=1}^k \varepsilon_u$  is calculated as the total number of words minus the number of outliers in the manuscript and thresholded using  $t$ , which



is defined by  $v = k$  the total manuscript words and  $C = 0.2$ . So, the obtained value of the labeling function determines the consequent relative label describing the text size inconsistency as either ‘None’ or ranging from ‘Very low’ to ‘Very high.’

Finally, the overall manuscript is analyzed and characterized in terms of ‘Text complexity’ (C20) using the inverted grayscale image  $I'_{gray}$  after filtering out all non-textual components to represent only the pure textual content of the manuscript being processed. Uniform local binary pattern (ULBP) technique [4] is adapted and used to represent and analyze the degree of complexity of the handwritten text, as defined by Eqs. (14)–(16). This technique is implemented based on an LBP operator designed with  $P = 8$  neighbors symmetrically distributed along the circumference of a circle of radius  $R = 1$ , note that <sup>riu2</sup> signifies the rotation invariance of uniform LBP to have two transitions at most. This implies that if an evaluated  $3 \times 3$  pattern satisfies  $U \leq 2$ , it is considered a uniform pattern and, as in Eq. (14), it is assigned a label from all possible nine unique labels ranging from 0 to 8 based on the number of ones in the ULBP, where these nine labels summarize all possible 58 decimal values of the same ULBP in different rotations; otherwise the pattern is considered as a miscellaneous non-uniform pattern and labeled with  $(P + 1) = 9$ . The number of transitions is computed by Eq. (15) for all eight neighbors from  $g_0$  to  $g_{P-1}$ , where each neighbor’s gray value  $g_p$  is thresholded by its difference with the center pixel’s gray value  $g_c$  computed as  $x = g_p - g_c$  and then assigned for  $s(x)$  either 1 when  $g_p \geq g_c$  and 0 when  $g_p < g_c$ , as defined in Eq. (16).

$$LBP_{P,R}^{riu2} = \begin{cases} \sum_{p=0}^{P-1} s(g_p - g_c) & \text{if } U(LBP_{P,R}) \leq 2 \\ P + 1 & \text{otherwise} \end{cases} \quad (14)$$

where

$$U(LBP_{P,R}) = |s(g_{P-1} - g_c) - s(g_0 - g_c)| + \sum_{p=1}^{P-1} |s(g_p - g_c) - s(g_{p-1} - g_c)| \quad (15)$$

where

$$s(g_p - g_c) = s(x) = \begin{cases} 1 & \text{if } x \geq 0 \\ 0 & \text{if } x < 0 \end{cases} \quad (16)$$

Thus, the text complexity characteristic is attained using Eqs. (11) and (12) such that  $f(x)$  is computed as the pixel sum of the produced ULBP image, and the multi-scale threshold  $t$  is defined by  $C = 0.2$ , and a value of  $v$  derived as the pixel sum of a thresholding ULBP image. The thresholding ULBP image is obtained by creating a binary mask of the convex hull per object for all content of the manuscript image  $I$  being processed to be, in turn, used for masking a synthetic random grayscale image generated as random noise imitating a very complex counterpart of the same manuscript content. Then, the ULBP is computed for the masked image, and the ULBP sum is assigned to  $v$  and used with  $C$  to characterize the multi-scale thresholding. As such, proper absolute and relative labels are assigned accordingly based on a pre-trained multi-scale thresholding model defining the corresponding numeral range of each relative label for semantically characterizing overall text complexity in a manuscript.

## 4 Semantic-Based Clustering and Retrieval

### 4.1 Semantic Characteristic-Based Manuscript Clustering

It is a practical use of the proposed semantic layout characteristics to successfully attain a beneficial and meaningful manuscript clustering based on their semantic characteristic similarities. In such an unsupervised learning task and among a variety of functional techniques of clustering

validity measurement [47], the Davies-Bouldin index (DBI) method is used to suggest an optimal number of clusters for partitioning the manuscript data into reasonable and separable groups. The DBI method is used along with  $k$ -means in such a way as to consider the advantages of both internal, besides external cluster evaluation schemes [48,49] to minimize intra-cluster and maximize inter-cluster distances, resulting in optimal  $k$ -number selection and better manuscript clustering. Thereby, after extensive and iterative evaluation of different  $k$  sizes ranging from 2 to 100,  $k=24$  continuously receives the smallest DBI and is, therefore, suggested as an optimal  $k$  number of clusters for better cluster configurations, as shown and compared with other 49 evaluated  $k$  values in Fig. 7. Thus, the optimal suggested 24-means are used for clustering all manuscripts in the database based on semantic layout characteristic similarities, as illustrated in Fig. 8.

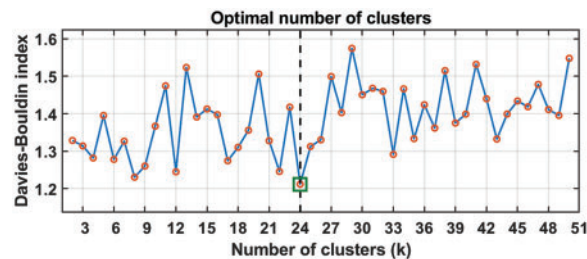


Figure 7: Davies-Bouldin clustering validation of different  $k$ -means

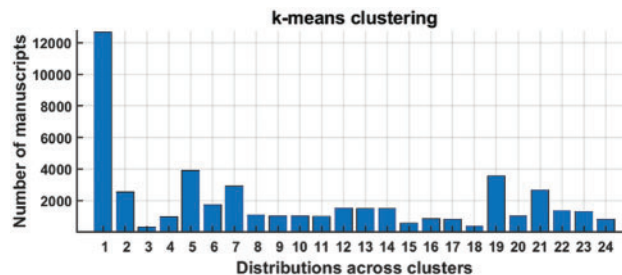


Figure 8:  $k$ -means clustering of manuscript data

#### 4.2 Semantic Characteristic-Based Manuscript Retrieval

The capability of manuscript retrieval based on semantic layout similarities is investigated, and the retrieval performance is evaluated and compared using different proposed combinations of semantic layout characteristics and physical features. Their performance is further explored and compared for their counterpart (physical features) derived by SDLA simultaneously to each semantic characteristic as vision-based metadata when used and added as supplemental features to the semantic characteristics. All *gallery* and *query* samples are analyzed and characterized via SDLA to obtain the required semantic characteristics and accompanying (metadata) physical features. Note that in the current experimental context, for a query manuscript image sample  $I_{query}$ , the more similar the retrieved manuscript's layout, the more precise the retrieval.

For achieving retrieval performance evaluation, 454 manuscript image samples from all 114 groups (Surahs) in all five categories/datasets (i.e., Dataset-1 to Dataset-5) are randomly selected and excluded to be used as a *query* subset to probe a *gallery* comprising all remaining manuscripts using

four different approaches for retrieval. These approaches incorporate the top-performing combinations of semantic characteristics and physical features, which are used to compose four types of feature vectors for gallery data and correspondingly for query data, as follows: *SemAbs-14* consists of 14 absolute semantic characteristics; *SemRel&PhysFtr-35* consists of 15 relative semantic characteristics in addition to 20 physical feature values corresponding to the 20 semantic characteristics; *SemAll-29* combines all 29 semantic characteristics including both 14 absolute and 15 relative characteristics; *SemAll&PhysFtr-49* is the combination of all 29 semantic absolute/relative characteristics and 20 physical features.

In this retrieval evaluation, suitable binary similarity (or relevance) metrics [32,50–52] are adopted and redefined to suit the current context and used based on the ground truth that classifies each query sample to one of the 24 determined  $k$ -means or clusters in the semantic characteristic space, such that a retrieved gallery sample is considered as a true positive ( $tp$ ) sample only if it belongs to the actual cluster of the query sample. Otherwise, it is considered as a false positive ( $fp$ ) sample, and, therefore, all missed (positive) samples belonging to the actual cluster and supposed to be retrieved from the gallery are considered false negative ( $fn$ ) samples. Min-max normalization is applied to both gallery and query samples using the minimum and maximum values of only gallery (training) data. As such, different retrieval evaluation metrics are inferred, including precision ( $P$ ), recall ( $R$ ), and F-measure ( $F$ ), which can be expressed as follows:

$$P = \frac{tp}{tp + fp} = \frac{\text{Similar-layout manuscripts retrieved}}{\text{Total manuscripts retrieved from the gallery}} \quad (17)$$

$$R = \frac{tp}{tp + fn} = \frac{\text{Similar-layout manuscripts retrieved}}{\text{Overall similar-layout manuscripts in the gallery}} \quad (18)$$

$$F = \frac{2 * P * R}{P + R} \quad (19)$$

In addition to three additional consequent mean-averaged metrics deduced as mean average precision ( $MAP$ ), mean average recall ( $MAR$ ), and mean average F-measure ( $MAF$ ), which can be formulated as follows:

$$MAP = \frac{1}{Q} \sum_{i=1}^Q AP_i, \text{ where } AP = \frac{1}{S} \sum_{j=1}^S P_j \quad (20)$$

$$MAR = \frac{1}{Q} \sum_{i=1}^Q AR_i, \text{ where } AR = \frac{1}{K} \sum_{j=1}^K R_j \quad (21)$$

$$MAF = \frac{1}{Q} \sum_{i=1}^Q AF_i, \text{ where } AF = \frac{1}{K} \sum_{j=1}^K F_j \quad (22)$$

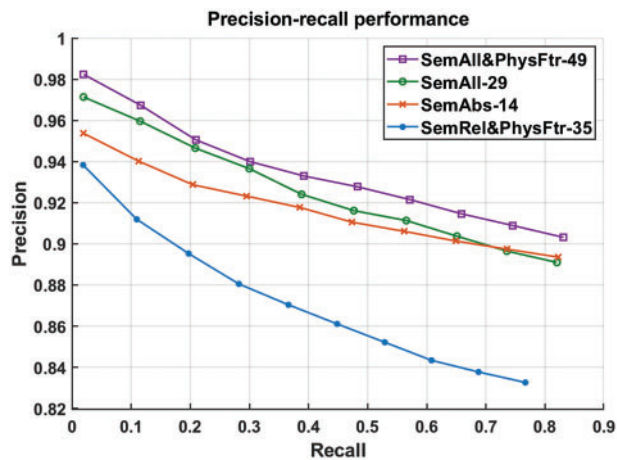
where  $Q$  is the total number of queries for retrieval evaluation,  $K$  denotes the current rank quantifying the number of top  $K$  retrieved items for a given query, and  $S$  is the number of retrieved manuscripts only with (relevant) similar layouts, which is used for averaging the sum of all  $P_j$  precisions, where  $S \leq K$ .

Table 3 reports the retrieval performance with respect to  $MAP$ ,  $MAR$ , and  $MAF$  measurements deduced for the four proposed semantic approaches (*SemAbs-14*, *SemRel&PhysFtr-35*, *SemAll-29*, and *SemAll&PhysFtr-49*). *SemAll&PhysFtr-49* receives the highest scores in all measurements, indicating the best possible retrieval capability attained by the total capacity of proposed semantic characteristics and supplemental physical features. The *SemAll-29* approach gains the second-best

performance with a smaller number of features comprising solely semantic characteristics, emphasizing their potency even when used alone for retrieval. The approach merely using all absolute characteristics, *SemAbs-14*, outperforms the approach of *SemRel&PhysFtr-35*, which uses all relative characteristics even when supplemented by physical features. Fig. 9 shows that all approaches start with high precision for retrieval ranging from 94% to 98%, where the best precision-recall performance is consistently demonstrated by *SemAll&PhysFtr-49*, followed by the other approaches in the same order of performance, in compliance with Table 3.

**Table 3:** Performance of semantic characteristic-based manuscript retrieval

Retrieval approach	Precision ( <i>MAP</i> )	Recall ( <i>MAR</i> )	F-measure ( <i>MAF</i> )
<i>SemAbs-14</i>	0.935	0.462	0.566
<i>SemRel&amp;PhysFtr-35</i>	0.890	0.439	0.538
<i>SemAll-29</i>	0.936	0.463	0.568
<i>SemAll&amp;PhysFtr-49</i>	<b>0.943</b>	<b>0.469</b>	<b>0.575</b>



**Figure 9:** Precision vs. recall measures of semantic retrieval performance

#### 4.3 Top-k Retrieval Using Semantic Layout Characteristics

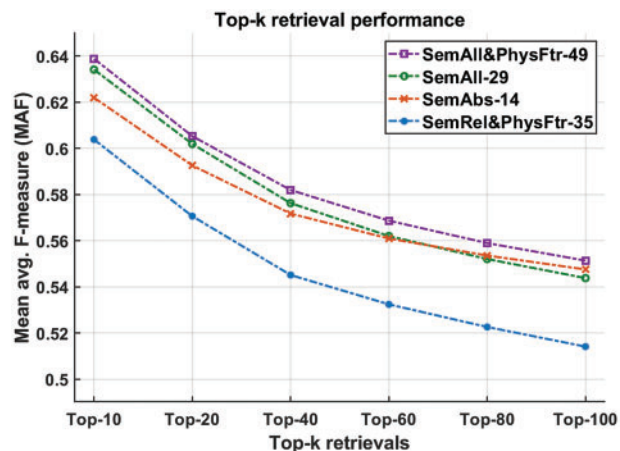
Top- $k$  retrieval is a highly potential practical application where proposed SDLA may be conducted, and resulting semantic layout characteristics can be enforced for different classification, match, search, and retrieval purposes. Thus, as a proof of concept, the four proposed semantic approaches, along with the same *query* subset described in Section 4.2, are used here for conducting several experiments to retrieve top- $k$  similar manuscripts where  $k$  is set to 10, 20, 40, 60, 80, and 100 consecutively throughout experiments, where retrieval is achieved based on semantic characteristic-based layout similarities. Hence, for a query manuscript image sample  $I_{query}$ , the more similar the top- $k$  retrieved manuscripts' layout, the more precise the retrieval.

Table 4 and Fig. 10 summarize and illustrate the variation and comparison of retrieval performance in terms of F-measure inferred with different top- $k$  retrievals. Furthermore, the average *MAF* value of all scores of *MAF* per top- $k$  is computed for each approach to conclude overall

performance/rank. As can be observed in Table 4, the retrieval performance may vary by changing the number of retrieved top- $k$  manuscripts. For instance, although *SemAll-29* achieves higher overall rank and performance than *SemAbs-14* with respect to average *MAF* and *MAF* scores of top- $k$  from 10 to 60, the performance of *SemAbs-14* exceeds the performance of *SemAll-29* in *MAF* scores of top- $k$  from 80 to 100. This can also be remarked in Fig. 10, where the *SemAbs-14* curve overcomes the curve and performance of *SemAll-29* at some point between 60 and 80 up to 100.

**Table 4:** Mean average F-measure (*MAF*) at different top- $k$  semantic retrievals

Retrieval approach	Top-10	Top-20	Top-40	Top-60	Top-80	Top-100	Avg. <i>MAF</i>	Overall Rank
<i>SemAbs-14</i>	0.622	0.593	0.572	0.561	0.554	0.548	0.575	3
<i>SemRel&amp;PhysFtr-35</i>	0.604	0.571	0.545	0.532	0.523	0.514	0.548	4
<i>SemAll-29</i>	0.634	0.602	0.576	0.562	0.552	0.544	0.578	2
<i>SemAll&amp;PhysFtr-49</i>	<b>0.639</b>	<b>0.605</b>	<b>0.582</b>	<b>0.569</b>	<b>0.559</b>	<b>0.551</b>	<b>0.584</b>	<b>1</b>



**Figure 10:** Mean average F-measure (*MAF*) of semantic retrieval performance along top- $k$  increase

## 5 Conclusions

Semantic document layout characteristics can be utilized as highly effective descriptions and ancillary information for analyzing and characterizing a complex structured handwritten document or manuscript. Such high-level semantic characteristics can offer additional advantages over the standard low-level layout features inferred by traditional DLA approaches and provide (human-friendly) more understandable and less confusable document analysis, besides more invariant labeling and characterization for successful layout similarity-based clustering and retrieval. In this research study, with a view to bridging the semantic gap, the extended SDLA approach is proposed and conducted, and the capabilities of the nascent semantic characteristics are investigated and evaluated. Even in case of imperfect detections or segmentations using physical layout analysis, the proposed semantic-based layout analysis and characterization can still assign accurate semantic layout characteristics, as they are observed to be more invariant and immune to potential minor errors or imperfect processes in the corresponding physical DLA.



The observed retrieval performance comparisons emphasize that the proposed semantic characteristics have different latent capabilities from the physical features. Nevertheless, they are found to be viable for high-performance retrieval when used alone, and they can offer additional potency for even higher performance when combined interacting with their counterpart physical features. Furthermore, the overall high-performance results of semantic characteristic-based clustering and retrieval on a large dataset of Arabic handwritten manuscripts with complex layouts suggest that the capability of semantically analyzing a document layout may pave the way for a variety of potential applications and future explorations.

This research work as an initial investigation was conducted using a single largescale dataset, which was limited to comprising only Arabic handwritten manuscripts. Thus, among several likely future research investigations, the proposed SDLA can be applied to different handwritten manuscript/document datasets in different languages, allowing for further performance comparison and generalization investigation. Moreover, the observed efficacy of the proposed SDLA approach and the capabilities of the proposed semantic layout characteristics can be exploited for automating many practical, real-life tasks, such as effort estimation and pricing of transcription or typing of complex handwritten manuscripts. Additionally, deep learning techniques may be adopted and used to learn a semantic characteristic-centric of document layouts.

**Acknowledgement:** The author would like to thank King Abdulaziz University Scientific Endowment for funding the research reported in this paper. The author would also like to thank Mr. Adel Turkistani, the editor-in-chief of the non-publicly available data source of the (preprint) Interpretation Encyclopedia of the Holy Quran, for providing the valuable large dataset of scanned manuscripts, which was used for conducting the experimental work of this research.

**Funding Statement:** This research was supported and funded by KAU Scientific Endowment, King Abdulaziz University, Jeddah, Saudi Arabia.

**Conflicts of Interest:** The authors declare that they have no conflicts of interest to report regarding the present study.

## References

- [1] G. M. Binmakhashen and S. A. Mahmoud, "Document layout analysis: A comprehensive survey," *ACM Computing Surveys (CSUR)*, vol. 52, no. 6, pp. 1–36, 2019.
- [2] S. Bhowmik, S. Kundu and R. Sarkar, "BINYAS: A complex document layout analysis system," *Multimedia Tools and Applications*, vol. 80, no. 6, pp. 1–34, 2020.
- [3] S. Mao, A. Rosenfeld and T. Kanungo, "Document structure analysis algorithms: A literature survey," in *Document Recognition and Retrieval X*, Santa Clara, California, USA: SPIE, pp. 197–207, 2003.
- [4] S. Ghosh, D. Lahiri, S. Bhowmik, E. Kavallieratou and R. Sarkar, "Text/non-text separation from handwritten document images using LBP based features: An empirical study," *Journal of Imaging*, vol. 4, no. 4, pp. 57, 2018.
- [5] W. Qin, R. Elanwar and M. Betke, "Text and metadata extraction from scanned Arabic documents using support vector machines," *Journal of Information Science*, vol. 48, no. 2, pp. 268–279, 2022.
- [6] M. Lemaître, E. Grosicki, E. Geoffrois and F. Prêteux, "Layout analysis of handwritten letters based on textural and spatial information and a 2D markovian approach," in *Int. Conf. on Frontiers in Handwriting Recognition (ICFHR)*, Québec, Canada, vol. 182, 2008.

- [7] H. T. Tran, N. Q. Nguyen, T. A. Tran, X. T. Mai and Q. T. Nguyen, "A deep learning-based system for document layout analysis," in *2022 The 6th Int. Conf. on Machine Learning and Soft Computing*, Haikou, China, pp. 20–25, 2022.
- [8] F. Grijalva, E. Santos, B. Acuña, J. C. Rodríguez and J. C. Larco, "Deep learning in time-frequency domain for document layout analysis," *IEEE Access*, vol. 9, pp. 151254–151265, 2021.
- [9] R. Agombar, M. Luebbering and R. Sifa, "A clustering backed deep learning approach for document layout analysis," in *Int. Cross-Domain Conf. for Machine Learning and Knowledge Extraction*, Dublin, Ireland, pp. 423–430, 2020.
- [10] A. M. Namboodiri and A. K. Jain, "Document structure and layout analysis," in *Digital Document Processing*, London: Springer, pp. 29–48, 2007.
- [11] N. Vasilopoulos and E. Kavallieratou, "Complex layout analysis based on contour classification and morphological operations," *Engineering Applications of Artificial Intelligence*, vol. 65, pp. 220–229, 2017.
- [12] S. Ravichandra, S. Siva Sathya and S. Lourdu Marie Sophie, "Deep learning based document layout analysis on historical documents," in *Advances in Distributed Computing and Machine Learning*, Singapore: Springer, pp. 271–281, 2022.
- [13] V. Alabau, C. -D. Martínez-Hinarejos, V. Romero and A. -L. Lagarda, "An iterative multimodal framework for the transcription of handwritten historical documents," *Pattern Recognition Letters*, vol. 35, pp. 195–203, 2014.
- [14] R. Barman, M. Ehrmann, S. Clematide, S. A. Oliveira and F. Kaplan, "Combining visual and textual features for semantic segmentation of historical newspapers," *Journal of Data Mining & Digital Humanities*, vol. HistoInformatics, pp. 1–26, 2021. Based on the journal link: <https://jdmhdh.episciences.org/7097>
- [15] O. Kodym and M. Hradiš, "Page layout analysis system for unconstrained historic documents," in *16th Int. Conf. on Document Analysis and Recognition*, Lausanne, Switzerland, pp. 492–506, 2021.
- [16] E. Granell, L. Quirós, V. Romero and J. A. Sánchez, "Reducing the human effort in text line segmentation for historical documents," in *Int. Conf. on Document Analysis and Recognition*, Lausanne, Switzerland, pp. 523–537, 2021.
- [17] G. M. BinMakhashen and S. A. Mahmoud, "Historical document layout analysis using anisotropic diffusion and geometric features," *International Journal on Digital Libraries*, vol. 21, no. 3, pp. 1–14, 2020.
- [18] A. M. Hesham, M. A. Rashwan, H. M. Al-Barhamtoshy, S. M. Abdou, A. A. Badr *et al.*, "Arabic document layout analysis," *Pattern Analysis and Applications*, vol. 20, no. 4, pp. 1275–1287, 2017.
- [19] A. Baig, S. A. Al-Ma'adeed, A. Bouridane and M. Cheriet, "Automatic segmentation and reconstruction of historical manuscripts in gradient domain," *IET Image Processing*, vol. 12, no. 4, pp. 502–512, 2017.
- [20] V. P. Le, N. Nayef, M. Visani, J. -M. Ogier and C. De Tran, "Text and non-text segmentation based on connected component features," in *2015 13th Int. Conf. on Document Analysis and Recognition (ICDAR)*, Tunis, Tunisia, pp. 1096–1100, 2015.
- [21] S. Bhowmik and R. Sarkar, "Classification of text regions in a document image by analyzing the properties of connected components," in *2020 IEEE Applied Signal Processing Conf. (ASPCON)*, Kolkata, India, pp. 36–40, 2020.
- [22] T. A. Tran, I. S. Na and S. H. Kim, "Page segmentation using minimum homogeneity algorithm and adaptive mathematical morphology," *International Journal on Document Analysis and Recognition (IJDAR)*, vol. 19, no. 3, pp. 191–209, 2016.
- [23] B. Liebl and M. Burghardt, "An evaluation of DNN architectures for page segmentation of historical newspapers," in *2020 25th Int. Conf. on Pattern Recognition (ICPR)*, Virtual-Milano, Italy, pp. 5153–5160, 2021.
- [24] C. Finegan-Dollak and A. Verma, "Layout-aware text representations harm clustering documents by type," in *Proc. of the First Workshop on Insights from Negative Results in NLP*, Online, pp. 60–65, 2020.
- [25] C. -A. Boiangiu, D. -C. Cananau, B. Raducanu and I. Bucur, "A hierarchical clustering method aimed at document layout understanding and analysis," *International Journal of Mathematical Models and Methods in Applied Sciences*, vol. 2, no. 1, pp. 413–422, 2008.

- [26] S. Marinai, E. Marino and G. Soda, "Tree clustering for layout-based document image retrieval," in *Second Int. Conf. on Document Image Analysis for Libraries*, Lyon, France, pp. 245–253, 2006.
- [27] U. D. Dixit and M. Shirdhonkar, "A survey on document image analysis and retrieval system," *International Journal on Cybernetics & Informatics (IJCI)*, vol. 4, no. 2, pp. 259–270, 2015.
- [28] U. D. Dixit and M. Shirdhonkar, "Document image retrieval: Issues and future directions," in *2021 Int. Conf. on Computational Intelligence and Computing Applications (ICCICA)*, Nagpur, India, pp. 1–4, 2021.
- [29] D. Sharma, G. Harit and C. Chattopadhyay, "Attributed paths for layout-based document retrieval," in *Workshop on Document Analysis and Recognition*, Hyderabad, India, pp. 15–26, 2018.
- [30] R. Jain, D. W. Oard and D. Doermann, "Scalable ranked retrieval using document images," in *Document Recognition and Retrieval XXI*, Singapore, San Francisco, CA, USA: SPIE, vol. 9021, pp. 179–193, 2014.
- [31] L. Denoue, S. Carter, J. Marlow and M. Cooper, "DocHandles: Linking document fragments in messaging apps," in *Proc. of the 2017 ACM Symp. on Document Engineering*, Valletta, Malta, pp. 81–84, 2017.
- [32] P. Zhang, C. Li, L. Qiao, Z. Cheng, S. Pu *et al.*, "VSR: A unified framework for document layout analysis combining vision, semantics and relations," in *Int. Conf. on Document Analysis and Recognition*, Lausanne, Switzerland, pp. 115–130, 2021.
- [33] V. Atanasiu, "The structural information potential and its application to document triage," *IEEE Access*, vol. 10, pp. 13103–13138, 2021.
- [34] R. S. Howyan and E. S. Jaha, "Semantic human face analysis for multi-level age estimation," *Intelligent Automation and Soft Computing*, vol. 31, no. 1, pp. 555–580, 2022.
- [35] H. Kwaśnicka and L. C. Jain (Eds.), "Bridging the semantic gap in image and video analysis," in *Image and Video Analysis*, vol. 145, Berlin: Springer, 2018.
- [36] W. Hu, Y. Sheng and X. Zhu, "A semantic image retrieval method based on interest selection," *Wireless Communications and Mobile Computing*, vol. 2022, pp. 1–6, 2022.
- [37] S. Lai, Q. Yang, W. He, Y. Zhu and J. Wang, "Image retrieval method combining bayes and SVM classifier based on relevance feedback with application to small-scale datasets," *Tehnički Vjesnik*, vol. 29, no. 4, pp. 1236–1246, 2022.
- [38] R. Youssef, H. Bouhadoun, J. D. Laredo and C. Chappard, "Semi-automatic compartment extraction to assess 3D bone mineral density and morphometric parameters of the subchondral bone in the tibial knee," in *2015 19th Int. Conf. on Information Visualisation*, Barcelona, Spain, pp. 518–523, 2015.
- [39] J. Fabrizio, "A precise skew estimation algorithm for document images using KNN clustering and Fourier transform," in *2014 IEEE Int. Conf. on Image Processing*, Paris, France, pp. 2585–2588, 2014.
- [40] T. Malisiewicz, A. Gupta and A. A. Efros, "Ensemble of exemplar-svms for object detection and beyond," in *2011 Int. Conf. on Computer Vision*, Barcelona, Spain, pp. 89–96, 2011.
- [41] R. Kabir, Y. Watanobe, M. R. Islam, K. Naruse and M. M. Rahman, "Unknown object detection using a one-class support vector machine for a cloud-robot system," *Sensors*, vol. 22, no. 4, pp. 1352, 2022.
- [42] S. Amraee, A. Vafaei, K. Jamshidi and P. Adibi, "Abnormal event detection in crowded scenes using one-class SVM," *Signal, Image and Video Processing*, vol. 12, no. 6, pp. 1115–1123, 2018.
- [43] G. P. C. Fung, J. X. Yu, H. Lu and P. S. Yu, "Text classification without negative examples revisit," *IEEE Transactions on Knowledge and Data Engineering*, vol. 18, no. 1, pp. 6–20, 2005.
- [44] Y. Wang, J. Wong and A. Miner, "Anomaly intrusion detection using one class SVM," in *Proc. from the Fifth Annual IEEE SMC Information Assurance Workshop*, West Point, NY, USA, pp. 358–364, 2004.
- [45] É. Puybareau and T. Géraud, "Real-time document detection in smartphone videos," in *2018 25th IEEE Int. Conf. on Image Processing (ICIP)*, Athens, Greece, pp. 1498–1502, 2018.
- [46] A. Lawgali, A. Bouridane, M. Angelova and Z. Ghassemlooy, "Automatic segmentation for Arabic characters in handwriting documents," in *18th IEEE Int. Conf. on Image Processing*, Athens, Greece, pp. 3529–3532, 2011.
- [47] C. Legány, S. Juhász and A. Babos, "Cluster validity measurement techniques," in *Proc. of the 5th WSEAS Int. Conf. on Artificial Intelligence, Knowledge Engineering and Databases*, Madrid, Spain, pp. 388–393, 2006.

- [48] A. K. Singh, S. Mittal, P. Malhotra and Y. V. Srivastava, "Clustering evaluation by Davies-Bouldin index (DBI) in cereal data using k-means," in *2020 Fourth Int. Conf. on Computing Methodologies and Communication (ICCMC)*, Erode, India, pp. 306–310, 2020.
- [49] M. Mughnyanti, S. Efendi and M. Zarlis, "Analysis of determining centroid clustering x-means algorithm with davies-bouldin index evaluation," in *IOP Conf. Series: Materials Science and Engineering*, Ulaanbaatar, Mongolia, pp. 1–6, 2020.
- [50] I. Mehmood, A. Ullah, K. Muhammad, D. -J. Deng, W. Meng *et al.*, "Efficient image recognition and retrieval on IoT-assisted energy-constrained platforms from big data repositories," *IEEE Internet of Things Journal*, vol. 6, no. 6, pp. 9246–9255, 2019.
- [51] M. Sajjad, A. Ullah, J. Ahmad, N. Abbas, S. Rho *et al.*, "Integrating salient colors with rotational invariant texture features for image representation in retrieval systems," *Multimedia Tools and Applications*, vol. 77, no. 4, pp. 4769–4789, 2018.
- [52] D. O'Sullivan, E. McLoughlin, M. Bertolotto and D. Wilson, "Context-oriented image retrieval," in *Int. and Interdisciplinary Conf. on Modeling and Using Context*, Paris, France, pp. 339–352, 2005.